PARTICLE-IN-CELL SIMULATION OF ELECTRON-HELIUM PLASMA IN CYCLOTRON GAS STOPPER[*]

Y.K. Batygin[#], G. Bollen, C. Campbell, F. Marti, D.J. Morrissey, G. Pang, S. Schwarz, NSCL,
Michigan State University, East Lansing, MI 48824, USA

Abstract

The cyclotron gas stopper is a newly proposed device to stop energetic rare isotope ions from projectile fragmentation reactions in a helium-filled chamber [1, 2]. The radioactive ions are slowed down by collisions with a buffer gas inside a cyclotron-type magnet and are extracted via interactions with a Radio Frequency (RF) field applied to a sequence of concentric electrodes (RF carpet). The present study focuses on a detailed understanding of space charge effects in the ion extraction region. The space charge is generated by the ionized helium gas created by the stopping of the ions and eventually limits the beam rate. Particle-in-cell simulations of a two-component (electron-helium) plasma interacting via Coulomb forces were performed in the space charge field created by the stopping beam.

INTRODUCTION

The cyclotron gas stopper is a device for the deceleration of radioactive ions created by the projectile fragmentation (see Fig. 1). Fast ions (~100 MeV/u) are injected into a helium-filled chamber inside a vertical magnetic field where they immediately enter a solid degrader so that they can be captured by the magnetic field. The fast ions lose the remainder of their kinetic energy in collisions with the helium buffer gas. This process ionizes the helium atoms. An electric field parallel to the magnetic field is used to remove electrons and move positively charged ions to the RF-carpet. At high incoming particle rates, the amount of ionization becomes so large that the stopped ions cannot be completely removed. As a result, a neutralized plasma accumulates in the center of the stopping chamber and additional fast ions are not or are only slowly extracted because they come to rest in the plasma-shielded region. This present work analyzed the overall process of charge migration to provide estimates of ion stopping efficiency as a function of incoming particle rate.

NUMERICAL METHOD

Present simulations are based on a preceding detailed numerical study of rare isotope production, transport, and stopping in a gas-filled magnetic field [1]. The program LISE++ [3] was used to calculate the transmission, yields, and ion-optical properties of the projectile fragment beam. A C++ version of the ATIMA code [4]

was used to calculate the energy lost by the incoming beam in the solid degrader. The Stopping and Range Tables from the SRIM package [5] were used to calculate the energy loss in the helium gas. The CycStop code [6] combined this input to calculate the fast ion stopping
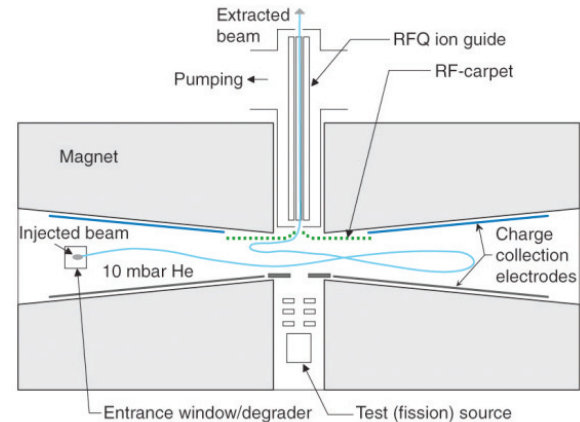

Figure 1: Schematic layout of cyclotron gas stopper [1]. The fast projectile fragments are incident horizontally at the left and after stopping are moved to the center for axial extraction.
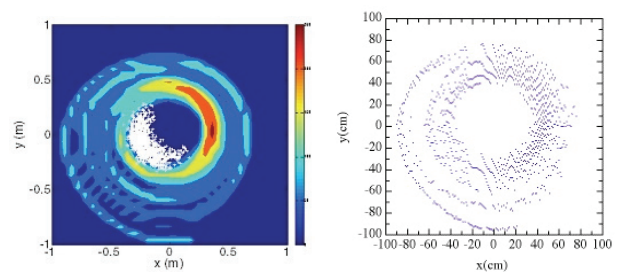

Figure 2: (Left) Top view of the energy loss density in color and the positions of the stopped ions in white, and (right) the distribution of e^-/He^+ ion-pairs created by the stopping of a ^{79}Br beam from the CycStop code [6].

distribution, the losses, and the spatial deposition of energy in the helium. The energy distributions were the input for the space charge phenomena in the present work (see Fig. 2).

The calculation of space charge effects in e^-/He^+ plasma were performed with a modified version of the BEAMPATH code [7]. The simulations were performed by simultaneous tracking of He^+ and electrons in the field created by their own space charge forces, $\vec{E}_{sc}$, and applied external electric field, $\vec{E}_o$, with a velocity $\vec{v}$ given by

$$\vec{v} = k(\vec{E}_o + \vec{E}_{sc}),$$ (1)

where k is the mobility of ion or electron. The mobility of He^+ ions at room temperature and pressure of $P = 200$ mbar was taken as $k_{He+} = 10^5$ cm^2/(kVs) and is inversely proportional to gas pressure. The mobility of electrons is typically three orders of magnitude higher than that of He^+ under the same conditions. However, direct simulation of e^-/He^+ plasma with such large differences in ion mobilities is problematic due to the dramatic difference in the time scales of the dynamics of electrons and He^+. Therefore, in the present work the mobility of the electrons was artificially reduced by a factor or ten to 10^7 cm^2/(kVs) to simultaneously follow the motion of the ions and electrons in the same calculation.

Radioactive ions were injected into the gas at a rate of dN/dt_{in}. Each incoming radioactive ion created a cloud of He^+ and electron charge at the rate dQ/dN, each. The product of these two rates gives the rate of creation of He^+ and electrons in the gas-filled chamber $dQ/dt = (dN/dt_{in})(dQ/dN)$. The simulation time step, $\Delta t = \Delta T/N_{step}$, was defined as a ratio of the simulation period, ΔT, and the number of integration steps, N_{step}. At each integration step the entire spatial distribution of e^-/He^+ particles was injected into the system such that the incoming charge of each component was $\Delta q = (dQ/dt)\, \Delta t$. This distribution is added to that remaining from the previously injected particles (see Fig. 3). The electrons and positive ions move in opposite directions in the net field created by applied collection field and by their space charge.

Space charge field is calculated via solution of Poisson's equation in two-dimensional cylindrical coordinates:

$$\frac{1}{r}\frac{\partial}{\partial r}(r\frac{\partial U}{\partial r}) + \frac{\partial^2 U}{\partial z^2} = Q(r, z), \qquad (2)$$

where $Q(r, z) = -\rho(r, z)/\varepsilon_o$ with Dirichlet boundary conditions at the surface of a tube of radius a, and Neumann condition at the axis:

$$U(a, z) = 0, \quad U(r, 0) = U(r, L) = 0, \quad \frac{\partial U}{\partial r}(0, z) = 0. \quad (3)$$

In Eq. (2), Q is the total instantaneous value of charge of electrons and ions presented in the system. While at every time step, the new fraction of e^-/He^+ is injected into the system, some fraction of particles is removed through the extraction region and through the walls of the gas cell. The Poisson's equation (2) is substituted by finite-difference analog:

$$U_{k, j+1}(1 + \frac{1}{2(j-1)}) - 2U_{k, j}(1 + \frac{h_r^2}{h_z^2}) + U_{k, j-1}(1 - \frac{1}{2(j-1)})$$

$$+ U_{k+1, j}(\frac{h_r}{h_z})^2 + U_{k-1, j}(\frac{h_r}{h_z})^2 = -Q_{k, j}h_r^2. \qquad (4)$$

Poison's equation is solved via Fourier transformation in z-direction and solution of three-diagonal matrix equation in radial direction. Accuracy of calculations is controlled by calculation of error of the Gauss theorem

$$\vartheta = 1 - \left| \int_S \vec{E}\, d\vec{S} / \int_v Q\, dv \right|, \qquad (5)$$

which is usually of the order of 10^{-3} (see Fig.4).

SIMULATION RESULTS

Fig. 3 illustrates the dynamics of e^-/He^+ cloud formation for the injection of ^{79}Br ions into the system with an axial electric field of $E_o=10$ V/cm for an incoming particle rate of $dN/dt_{in} = 10^5$ part/sec and energy of $E = 1.69\cdot10^9$ eV. The number of e^-/He^+ pairs per stopped ion is $N = E / E_i = 4.23\cdot10^7$ where $E_i = 40$ eV is the effective ionization potential in helium gas. Each incoming beam particle creates e^-/He^+ pairs equal to $dQ/dN = 6.76\cdot10^{-12}$ C/part so that the increase in charge due to e^-/He^+ pairs in the system is $dQ/dt = 6.76\cdot10^{-7}$ C/s. As illustrated in Fig. 3, shortly after starting the injection of beam, the electrons quickly travel to the anode wall of gas cell at $z = 10$ cm (the right edge in this view). After $t = 5\cdot10^{-3}$ sec, the system has relaxed to steady-state condition for this beam rate. Under these conditions the outgoing particle rate is equal to incoming rate $dN/dt_{out} = dN/dt_{in}$. The charged particles are considered to be extracted from the gas if they reach the walls (anode or cathode used to apply the drift field).
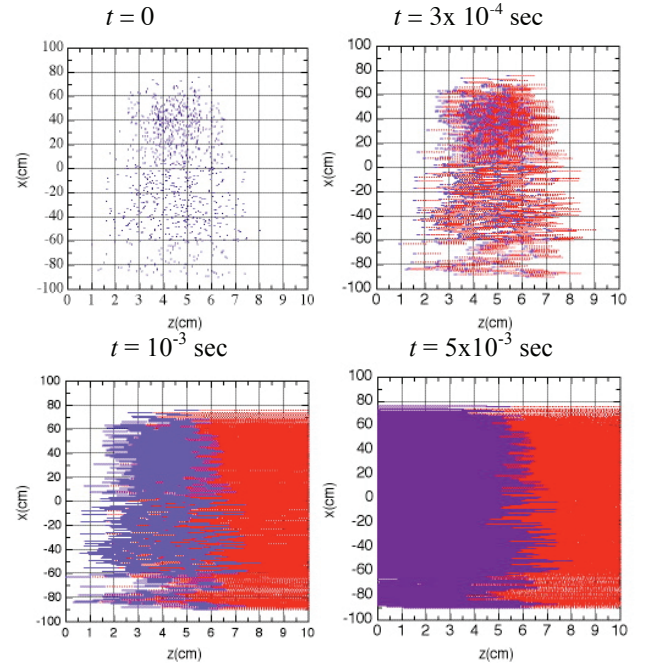

Figure 3: Time sequence of the motion of He^+ ions (blue) and e^- (red) created by a ^{79}Br beam at $dN/dt_{in}=10^5$ part/sec. The applied (horizontal) electric field was 10 V/cm.
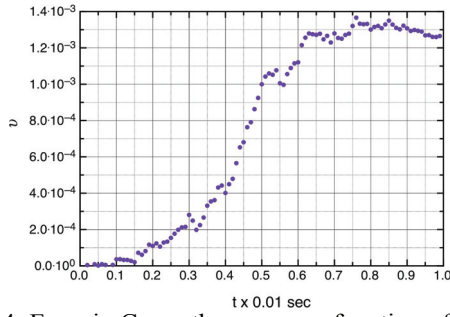
Figure 4: Error in Gauss theorem as a function of time.

Table 1: Simulation Parameters

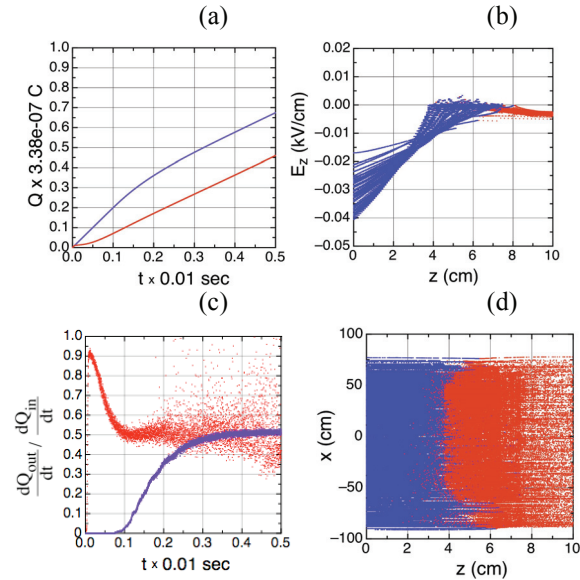|	
Energy per stopped ion	$1.69 \cdot 10^9$ eV
He^+ mobility coefficient	$k_{He+} = 10^5$ cm^2/kVs
e^- "mobility coefficient"	$k_e = 10^7$ cm^2/kVs
Number of macroparticles per filling	$2 \cdot 10^3$
Number of integration steps	$5 \cdot 10^3$
Total number of macroparticles	10^7
Box for Poisson's equation $R \times Z$	150 cm x 10 cm
Mesh $N_R \times N_Z$	1024 x 1024

Figure 5: Conditions for space-charge neutralized plasma with e^-(red) and He^+(blue) at incoming beam rate of $dN/dt_{in}=10^7$part/s: (a) accumulated charge, (b) total electric field, (c) flux of electrons through $z=0$ and that of $He+$ through $z=10$cm, (d) particle distribution at $t=5 \cdot 10^{-3}$s.

At significantly higher incoming beam rates, the fraction of outgoing ions becomes lower than the creation rate of ionized gas. This results from the formation of charged neutralized area in the regions of the chamber with the highest ionization densities (see Fig. 5). This limits the extraction of radioactive ions as well because some of the beam stops in the neutralized area and cannot leave the region. Fig. 5d illustrates the calculated motion of e^-/He^+ ions at an incoming particle rate of $dN/dt_{in}=10^7$ part/s. This problem becomes more pronounced with increasing incoming particle rate. Fig. 6 illustrate the dependence of extraction efficiency of e^-/He^+ ions as a

function of the incoming charge rate for different values of buffer gas pressure and applied electric field. The space charge forces were found to significantly limit the extraction efficiency when the incoming rate exceeded $dN/dt_{in} = 5 \cdot 10^6$ part/s.

The present calculations were used to estimate the total collection and extraction efficiency of radioactive beam from the cyclotron gas stopper. As a test, the actual spiral distribution of ionized buffer gas was replaced by a uniform disk of 75 cm radius, with an axial ionization distribution centered at $z = 5$ cm and $\sigma_z = 1.5$ cm. Both the actual and simple distributions give a similar dependence of the extraction efficiency on the incoming particle rate. The results for the extraction of e^-/He^+ ions were combined with the predicted stopping distribution of high energy ^{16}O ions in the cyclotron stopper to obtain a total efficiency for stopping and collection (see Fig. 7). The figure show the advantage of using a cyclotron gas stopper over a traditional linear gas stopper for high-intensity, light ion beams.

The present results should be considered with some caution due to the reduced electron mobility and the omission of any diffusion processes. Continued development of the cyclotron gas stopper design is underway including detailed studies of the effects of space charge on the ion motion at the RF-carpet and investigations into techniques to perform calculations with the true electron mobility.
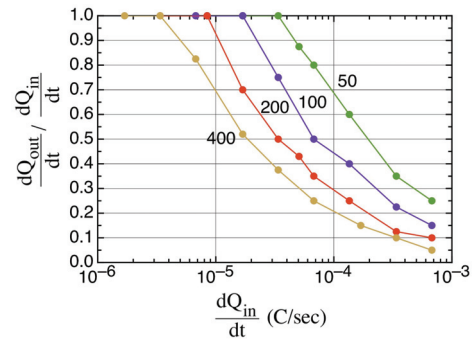

Figure 6: The fraction of extracted charge, i.e., efficiency of e^-/He^+ extraction, as a function of incident beam rate for different values of buffer gas pressure (in mbar).
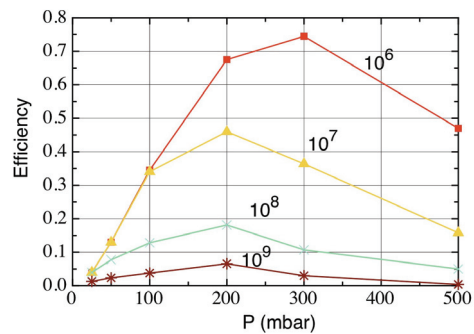

Figure 7: The total efficiency for ^{16}O heavy ions as a function of gas pressure and incident beam rate (in part/s).

REFERENCES

[1] G. Bollen, D.J. Morrissey, S. Schwarz, Nucl. Instrum. Meth. A550, (2005) 27.

[2] G.K.Pang, et. al, Proc. of PAC07, Albuquerque, New Mexico, USA (2007) 3588-3590.

[3] O.Tarasov and D.Bazin, Nucl. Phys. A746 (2004) 411.

[4] H. Weick, http://www-linux.gsi.de/~weick/atima/

[5] J.F. Ziegler, http://www.srim.org/

[6] C. Campbell, et al., Nucl. Instr. Meth. A, to be published.

[7] Y.Batygin, Nucl. Instrum. Meth. A539 (2005) 455.